

This discussion paper is/has been under review for the journal Natural Hazards and Earth System Sciences (NHESS). Please refer to the corresponding final paper in NHESS if available.

Classification of homoclinic rogue wave solutions of the nonlinear Schrödinger equation

A. R. Osborne

Nonlinear Waves Research Corporation, Arlington, Virginia, USA

Received: 20 August 2013 – Accepted: 24 August 2013 – Published: 29 January 2014

Correspondence to: A. R. Osborne (al.osborne@gmail.com)

Published by Copernicus Publications on behalf of the European Geosciences Union.

NHESSD

2, 897–933, 2014

Discussion Paper | Discussion Paper

Classification of
homoclinic rogue
wave solutions

A. R. Osborne

Title Page

Abstract

Introduction

Conclusions

References

Tables

Figures



Back

Close

Full Screen / Esc

Printer-friendly Version

Interactive Discussion



Abstract

Certain *homoclinic solutions* of the nonlinear Schrödinger (NLS) equation, with spatially periodic boundary conditions, are the most common *unstable wave packets* associated with the phenomenon of oceanic rogue waves. Indeed the homoclinic solutions due to

- 5 Akhmediev, Peregrine and Kuznetsov-Ma are almost exclusively used in scientific and engineering applications. Herein I investigate an infinite number of *other* homoclinic solutions of NLS and show that they reduce to the above three classical homoclinic solutions for particular spectral values in the periodic inverse scattering transform. Furthermore, I discuss another infinity of solutions to the NLS equation that are *not classifiable as homoclinic solutions*. These latter are the genus- $2N$ theta function solutions 10 of the NLS equation: they are the most general unstable *spectral solutions* for periodic boundary conditions. I further describe how the homoclinic solutions of the NLS equation, for $N = 1$, can be derived directly from the theta functions in a particular limit. The solutions I address herein are actual *spectral components* in the nonlinear Fourier 15 transform theory for the NLS equation: The periodic inverse scattering transform.

The main purpose of this paper is to discuss a broader class of rogue wave packets¹ for ship design, as defined in the Extreme Seas program. The spirit of this research came from D. Faulkner (2000) who many years ago suggested that ship design procedures, in order to take rogue waves into account, should progress beyond the use of 20 simple sine waves.

¹An overview of other work in the field of rogue waves is given elsewhere: Osborne 2010, 2012 and 2013. See the books by Olagnon and colleagues 2000, 2004 and 2008 for the Brest meetings. The books by Kharif et al. (2008) and Pelinovsky et al. (2010) are excellent references.

Classification of homoclinic rogue wave solutions

A. R. Osborne

Title Page

Abstract

Introduction

Conclusions

References

Tables

Figures

◀

▶

◀

▶

Back

Close

Full Screen / Esc

Printer-friendly Version

Interactive Discussion



1 The generalized rogue wave

The homoclinic solution to the NLS equation

$$iu_t + u_{xx} + 2|u|^2 u = 0$$

for *spatially periodic boundary conditions* ($u(x, t) = u(x + L, t)$) is given by (see Ablowitz and Clarkson, 1992):

$$u(x, t) = a \left(\frac{1 - 2\cos(Kx)e^{\Omega t - 2i\phi + \gamma} + Ae^{2\Omega t - 4i\phi + 2\gamma}}{1 - 2\cos(Kx)e^{\Omega t + \gamma} + Ae^{2\Omega t + 2\gamma}} \right) e^{2ia^2 t} \quad (1)$$

where

$$\Omega = K \sqrt{4a^2 - K^2} \quad (\text{Frequency}) \quad (2)$$

$$K = 2a \sin \phi \quad (\text{Wavenumber}) \quad (3)$$

$$L = \frac{2\pi}{K} = \frac{\pi}{a \sin \phi} \quad (\text{Wavelength}) \quad (4)$$

$$a = \sec^2 \phi = \frac{1}{\cos^2 \phi} \quad (5)$$

Here a is the amplitude of the carrier wave. Notice that the parameter γ may be interpreted as just a temporal phase shift and could just as well be omitted. However, I use γ to keep the maximum of the waveform at the origin, $u_{\max} = u(0, 0)$. The presence of

Title Page

Abstract

Introduction

Conclusions

References

Tables

Figures

◀

▶

◀

▶

Back

Close

Full Screen / Esc

Printer-friendly Version

Interactive Discussion



Classification of homoclinic rogue wave solutions

A. R. Osborne

[Title Page](#)

[Abstract](#)

[Introduction](#)

[Conclusions](#)

[References](#)

[Tables](#)

[Figures](#)

[|◀](#)

[▶|](#)

[◀](#)

[▶](#)

[Back](#)

[Close](#)

[Full Screen / Esc](#)

[Printer-friendly Version](#)

[Interactive Discussion](#)



the parameter ϕ is the only difference between the numerator and denominator and is fundamental for describing modulational solutions of the NLS equation (see Sect. 8 below).

Some observations are in order here with respect to relating the above solution the inverse scattering transform (IST) which I discuss further in Sect. 8. Clearly ϕ must be related to the *periodic IST eigenvalue*² in the so-called λ -plane, where the Floquet problem for the Zakharov-Shabat eigenvalue problem is solved. Recall that the wavenumber is related to λ by the following relation (this is just the IST loop integral to leading order in ε (see Sect. 8 and Osborne, 2010)):

$$K = 2\sqrt{a^2 + \lambda^2} \quad (6)$$

Here $\lambda = \lambda_R + i\lambda_I$, such that

$$\lambda_I = a \cos \phi, \quad \lambda_R = 0 \quad (7)$$

Then

$$K = 2\sqrt{a^2 - \lambda_I^2} = 2a\sqrt{1 - \cos^2 \phi} = 2a \sin \phi \quad (8)$$

So we have the wavenumber in the λ -plane eigenvalue and the relation $\lambda_I = a \cos \phi$ results. The frequency can be written

$$\begin{aligned} \Omega &= K \sqrt{4a^2 - K^2} = 2aK \sqrt{1 - \sin^2 \phi} \\ &= 2aK \cos \phi = 4a^2 \sin \phi \cos \phi = 2a^2 \sin(2\phi) = 2K\lambda_I \end{aligned} \quad (9)$$

Again, this latter result derives from the appropriate loop integral for ε small. Furthermore

$$A = \frac{1}{\cos^2 \phi} = \left(\frac{a}{\lambda_I}\right)^2 \quad L = \frac{2\pi}{K} = \frac{\pi}{a \sin \phi} = \frac{2\pi}{2\sqrt{a^2 - \lambda_I^2}} \quad (10)$$

²Associated with the Floquet problem for the Zakharov-Shabat eigenvalue problem.

Another nice relation is

$$\tan \phi = \frac{K}{2\lambda_I} = \frac{2\sqrt{a^2 - \lambda_I^2}}{2\lambda_I} \quad (11)$$

A geometric diagram of the λ -plane is shown in Fig. 1.³

Another interesting result relates to the parameter γ . If we write $\Omega t + \gamma = \Omega(t + \gamma/\Omega) = \Omega\tau$, for $\tau = (t + \gamma/\Omega)$, then the homoclinic solution becomes

$$u(x, \tau) = a \left(\frac{1 - 2\cos(Kx)e^{\Omega\tau - 2i\phi} + Ae^{2\Omega\tau - 4i\phi}}{1 - 2\cos(Kx)e^{\Omega\tau} + Ae^{2\Omega\tau}} \right) e^{2ia^2t} \quad (12)$$

This may be one of the most useful forms of the homoclinic solution, since γ does not appear directly as it results only in a temporal phase shift.

Hence, we have the general homoclinic solution of the NLS equation beneath the carrier on the imaginary axis of the lambda plane with all parameters inserted:

$$u(x, t) = a \left[\frac{1 - 2e^{\gamma - 2i\phi + 2a^2 \sin(2\phi)t} \cos(2a \sin \phi x) + \sec^2 \phi e^{2\gamma - 4i\phi + 4a^2 \sin(2\phi)t}}{1 - 2e^{\gamma + 2a^2 \sin(2\phi)t} \cos(2a \sin \phi x) + \sec^2 \phi e^{2\gamma + 4a^2 \sin(2\phi)t}} \right] e^{2ia^2t} \quad (13)$$

Note that ϕ is the IST phase and γ is seen in the role of an amplitude-multiplying factor in the initial modulation. Now set

$$\theta(t) = 2a^2 \sin(2\phi)t \quad (14)$$

³Note that Fig. 1 gives the geometry below the carrier, *i.e.* The equivalent geometry *above* the carrier is given in Fig. 7 below.

Classification of homoclinic rogue wave solutions

A. R. Osborne

Title Page

Abstract

Introduction

Conclusions

References

Tables

Figures

◀

▶

◀

▶

Back

Close

Full Screen / Esc

Printer-friendly Version

Interactive Discussion



so that

$$u(x, t) = a \left[\frac{1 - 2e^\gamma e^{\theta(t)-2i\phi} \cos(2a \sin \phi x) + e^{2\gamma} \sec^2 \phi e^{2\theta(t)-4i\phi}}{1 - 2e^\gamma e^{\theta(t)} \cos(2a \sin \phi x) + e^{2\gamma} \sec^2 \phi e^{2\theta(t)}} \right] e^{2ia^2 t} \quad (15)$$

The *primordial time*, corresponding to a small amplitude modulation, for this expression is given by (set $\varepsilon = e^{2a^2 \sin 2\phi t}$, and expand a Taylor series in ε as $t \rightarrow -\infty$):

5 $u(x, t) \approx a \left[1 + 4\varepsilon e^\gamma \sin \phi e^{i(\frac{\pi}{2}-\phi)} \cos(2a \sin \phi x) \right] e^{2ia^2 t} \quad (16)$

This expression is useful as an initial condition in a numerical experiment or (suitably modified from sNLS to tNLS) as a “paddle” motion in a laboratory experiment. More details are given in Osborne (2010).

2 An alternative expression for the rogue wave

10 Equation (15) can be rewritten in the following form:

$$u(x, t) = -a \left[\frac{\operatorname{Tanh}(2a^2 \sin 2\phi t) + e^{\gamma-2i\phi} \cos(2a \sin \phi x) \operatorname{Sech}(2a^2 \sin 2\phi t)}{1 - e^\gamma \cos(2a \sin \phi x) \operatorname{Sech}(2a^2 \sin 2\phi t)} \right] e^{2ia^2 t} \quad (17)$$

where

$$\operatorname{Tanh}(2a^2 \sin 2\phi t) \equiv - \left(\frac{e^{2\gamma} \sec^2 \phi e^{2\theta-4i\phi} + 1}{e^{2\gamma} \sec^2 \phi e^{2\theta} + 1} \right) \quad (18)$$

$$\operatorname{Sech}(2a^2 \sin 2\phi t) \equiv \left(\frac{2e^\theta}{1 + e^{2\gamma} \sec^2 \phi e^{2\theta}} \right)$$

15 This form of the *homoclinic rogue wave* is useful as we see below. Note that the function definitions “Tanh” and “Sech” are simple generalizations of the classical hyperbolic functions “tanh” and “sech”. For $e^{2\gamma} \sec^2 \phi = 1$ and $\phi = \pi/4$ these relationships are exact, providing simple special cases we now study.

Title Page

Abstract

Introduction

Conclusions

References

Tables

Figures

◀

▶

Back

Close

Full Screen / Esc

Printer-friendly Version

Interactive Discussion



3 The Akhmediev breather

This case takes the specific values (where $\lambda_1 = ia/\sqrt{2}$)

$$\phi = \frac{\pi}{4}, \quad \gamma = \frac{1}{2} \ln \left(\frac{1}{2} \right) \quad (19)$$

for which

$$e^{2i\phi} = i, \quad e^{4i\phi} = -1 \quad (20)$$
$$e^\gamma = \frac{\sqrt{2}}{2}, \quad e^{2\gamma} = \frac{1}{2}$$

and then Eq. (13) becomes the *Akhmediev breather* (Akhmediev, 1986):

$$u(x, t) = -ia \left[\frac{\cos(\sqrt{2}ax)\operatorname{sech}(2a^2t) + \sqrt{2}i\tanh(2a^2t)}{\sqrt{2} - \cos(\sqrt{2}ax)\operatorname{sech}(2a^2t)} \right] e^{2ia^2t} \quad (21)$$

which has the associated *primordial form*, $t \rightarrow -\infty$:

$$u(x, t) \approx -ia \left[1 + \sqrt{2}\varepsilon(1+i)\cos(\sqrt{2}ax) \right] e^{2ia^2t} \quad (22)$$

The extra factor of $-i$ just phase shifts the NLS solution by $-\pi/2$. A graph of this simple case is given in Fig. 2.

Note, further, that for the specific values of ϕ, γ in (19), when used in (17), clearly gives (21). This happens because in this case we have the simple reductions:

$$\operatorname{Tanh}(2a^2 \sin 2\phi t) = \tanh(2a^2 t) = \left(\frac{e^{4a^2 t} - 1}{e^{4a^2 t} + 1} \right) = \left(\frac{e^{2a^2 t} - e^{-2a^2 t}}{e^{2a^2 t} + e^{-2a^2 t}} \right) \quad (23)$$

$$\operatorname{Sech}(2a^2 \sin 2\phi t) = \operatorname{sech}(2a^2 \sin 2\phi t) = \left(\frac{2e^{2a^2 \sin 2\phi t}}{1 + e^{4a^2 \sin 2\phi t}} \right) = \left(\frac{2}{e^{-2a^2 \sin 2\phi t} + e^{2a^2 \sin 2\phi t}} \right)$$

Title Page

Abstract

Introduction

Conclusions

References

Tables

Figures

◀

▶

◀

▶

Back

Close

Full Screen / Esc

Printer-friendly Version

Interactive Discussion



4 A simpler case for the rogue wave

Now let's see if we can give a simpler generalization of (17). Go back to the form (15) and set

$$e^{2\gamma} \sec^2 \phi = 1 \quad (24)$$

- 5 This establishes a simple functional relationship between γ and ϕ (see Fig. 1). We get

$$u(x, t) = a \left[\frac{\operatorname{Tanh}(2a^2 \sin 2\phi t) - e^\gamma e^{-2i\phi} \cos(2a \sin \phi x) \operatorname{sech}(2a^2 \sin 2\phi t)}{1 - 2e^\gamma \cos(2a \sin \phi x) \operatorname{sech}(2a^2 \sin 2\phi t)} \right] e^{2ia^2 t} \quad (25)$$

where

$$\operatorname{Tanh}(\theta) = \frac{1 + e^{-4i\phi} e^{2\theta}}{1 + e^{2\theta}} \quad (26)$$

- 10 Note that from (12)

$$\gamma = \frac{1}{2} \ln(\cos \phi) \quad (27)$$

This gives

$$u(x, t) = a \left[\frac{\operatorname{Tanh}(2a^2 \sin 2\phi t) - e^{-2i\phi} \cos \phi \cos(2a \sin \phi x) \operatorname{sech}(2a^2 \sin 2\phi t)}{1 - 2 \cos \phi \cos(2a \sin \phi x) \operatorname{sech}(2a^2 \sin 2\phi t)} \right] e^{2ia^2 t} \quad (28)$$

The curve $\gamma = \ln(\cos \phi)$ is graphed in Fig. 2. For $\phi = \pi/4$ in (19) we get the previous result (21), the Akhmediev breather.

Title Page

Abstract

Introduction

Conclusions

References

Tables

Figures

◀

▶

◀

▶

Back

Close

Full Screen / Esc

Printer-friendly Version

Interactive Discussion



5 The highest rogue wave

The highest wave happens for the case $\phi \sim \Delta\phi \ll 1$. Let us examine this fully. The maximum amplitude occurs at $x = t = 0$, hence we compute from (17):

$$|u(0,0)|(\phi, \gamma) = \sqrt{1 + \frac{4e^\gamma \sin^2 2\phi}{1 + 2e^{2\gamma} - 4e^\gamma \cos^2 \phi + \cos 2\phi}} \quad (29)$$

- 5 In this expression, I have made clear the dependence on the arbitrary parameters (ϕ, γ) . To see where the maximum of this function occurs I graph in Fig. 4 $|u(0,0)|(\phi, \gamma)$ as a function of ϕ, γ . Note that the maximum occurs for $\gamma = 0$, so that

$$|\psi(0,0)|(\phi, 0) = \sqrt{5 + 4 \cos 2\phi} \quad (30)$$

- which is graphed in Fig. 5. While strictly speaking the maximum occurs for $\gamma = \phi = 0$,
10 note that (1) is indeterminate for $\phi = 0$, hence we take $\phi > 0$.

6 The Peregrine solution

Now take the limit when the spatial period goes to infinity and the wavenumber goes to 0. This happens when we let $\phi \rightarrow 0$. Here is the breather solution

$$u(x, t) = a \left[\frac{1 - 2e^{\gamma - 2i\phi + 2a^2 \sin(2\phi)t} \cos(2a \sin \phi x) + \sec^2 \phi e^{2\gamma - 4i\phi + 4a^2 \sin(2\phi)t}}{1 - 2e^{\gamma + 2a^2 \sin(2\phi)t} \cos(2a \sin \phi x) + \sec^2 \phi e^{2\gamma + 4a^2 \sin(2\phi)t}} \right] e^{2ia^2 t} \quad (31)$$

- 15 This expression can be put into the simple form

$$u(x, \tau) = a \left[\frac{1 - 2e^{-2i\phi + 2a^2 \sin(2\phi)\tau} \cos(2a \sin \phi x) + \sec^2 \phi e^{-4i\phi + 4a^2 \sin(2\phi)\tau}}{1 - 2e^{2a^2 \sin(2\phi)\tau} \cos(2a \sin \phi x) + \sec^2 \phi e^{4a^2 \sin(2\phi)\tau}} \right] e^{2ia^2 t} \quad (32)$$

Title Page

Abstract

Introduction

Conclusions

References

Tables

Figures

◀

▶

◀

▶

Back

Close

Full Screen / Esc

Printer-friendly Version

Interactive Discussion



where

$$\tau = \left(t + \frac{\gamma}{\Omega} \right) = \left(t + \frac{\gamma}{2a^2 \sin(2\phi)} \right) = t + \gamma_o \quad (33)$$

This results emphasizes the fact that the temporal phase shift depends not only on γ , but also on ϕ :

$$^5 \quad \gamma_o = \frac{\gamma}{2a^2 \sin(2\phi)} \quad (34)$$

The problem simplifies if we let $\gamma \rightarrow 0$. Then expand the numerator and denominator to *second order* in ϕ . One finds for the modulation term

$$\frac{(-3 + 16a^4\tau^2 + 4a^2(-4i\tau + x^2))\phi^2}{(1 + 16a^4\tau^2 + 4a^2x^2)\phi^2} \quad (35)$$

The terms ϕ^2 cancel and the final result is:

$$^{10} \quad u(x, t) = a \left[1 - \frac{4(1 + 4ia^2t)}{1 + 16a^4t^2 + 4a^2x^2} \right] e^{2ia^2t} \quad (36)$$

This is the Peregrine (1983) result. Together with other “rogue waves” solutions of this type seen in his numerical simulations, Peregrine often referred to “rogue waves” as a “sudden steep event.” If instead we keep γ finite then we have the phase shift:

$$\gamma_o \sim \frac{\gamma}{4a^2\phi} \quad (37)$$

¹⁵ which tends to infinity in the $\phi \rightarrow 0$ limit.

A graph of the Peregrine solution is given in Fig. 6.

Classification of homoclinic rogue wave solutions

A. R. Osborne

[Title Page](#)

[Abstract](#)

[Introduction](#)

[Conclusions](#)

[References](#)

[Tables](#)

[Figures](#)

◀

▶

◀

▶

[Back](#)

[Close](#)

[Full Screen / Esc](#)

[Printer-friendly Version](#)

[Interactive Discussion](#)



7 The homoclinic rogue wave above the carrier in the Lambda Plane: The Kuznetsov-Ma Breather

Let us now focus on the results of (1)-(5) and Fig. 2. For spectra *above the carrier* we have $ia \leq \lambda_i < \infty$, where we assume the eigenvalue lies on the imaginary axis. This implies that (6) has the form (use $\lambda = i\lambda_i$, $ia \leq \lambda_i < \infty$, and $\lambda_i = a \cos(i\phi) = a \cosh \phi$):

$$K \rightarrow 2\sqrt{a^2 + \lambda^2} = 2i\sqrt{\lambda_i^2 - a^2} = 2ia \sinh \phi \quad (38)$$

This suggests:

$$\begin{aligned} \Omega \rightarrow K \sqrt{4a^2 - K^2} &= 2ia \sinh \phi \sqrt{4a^2 + (2a \sinh \phi)^2} = \\ &= 2ia \left(2a \sinh \phi \sqrt{1 + \sinh^2 \phi} \right) = 4ia^2 \sinh \phi \cosh \phi = 2ia^2 \sinh(2\phi) \end{aligned} \quad (39)$$

All of this occurs if we make the transformations: $\phi \rightarrow i\phi$, followed by $K \rightarrow iK$ and $\Omega \rightarrow i\Omega$. Here is the resultant solution to NLS above the carrier:

$$u(x, t) = -ia \left(\frac{1 - 2\cos(iKx)e^{i\Omega t + 2\phi + \gamma} + Ae^{2i\Omega t + 4\phi + 2\gamma}}{1 - 2\cos(iKx)e^{i\Omega t + \gamma} + Ae^{2i\Omega t + 2\gamma}} \right) e^{2ia^2 t} \quad (40)$$

This is the Kuznetsov-Ma (Kuznetsov, 1977 and Ma, 1979) form of the homoclinic solution of the NLS equation above the carrier. The final parameters are:

$$\lambda_i = a \cosh \phi \quad (41)$$

15

$$K = 2a \sinh \phi \quad (42)$$

$$\Omega = 2a^2 \sinh(2\phi) \quad (43)$$

[Title Page](#)

[Abstract](#)

[Introduction](#)

[Conclusions](#)

[References](#)

[Tables](#)

[Figures](#)

◀

▶

◀

▶

[Back](#)

[Close](#)

[Full Screen / Esc](#)

[Printer-friendly Version](#)

[Interactive Discussion](#)



with the Kuznetsov-Ma (Kuznetsov, 1977 and Ma, 1979) solution:

$$u(x, t) = -ia \left(\frac{1 - 2\cosh(Kx)e^{i\Omega t + 2\phi + \gamma} + Ae^{2i\Omega t + 4\phi + 2\gamma}}{1 - 2\cosh(Kx)e^{i\Omega t + \gamma} + Ae^{2i\Omega t + 2\gamma}} \right) e^{2ia^2 t} \quad (44)$$

Figure 7. Geometry of parameters for a homoclinic, unstable mode above the carrier in the lambda plane, i.e. where λ_i lies on the interval (ia, ∞) .

A simpler analytical expression gives the Kuznetsov-Ma breather⁴, for which $\lambda_i = ia\sqrt{2}$. This means $\cosh\phi = \sqrt{2}$, $\sinh\phi = 1$ and $\phi = 0.88137$ degrees (Osborne, 2010). Here $K = 2a \sinh\phi = 2a$ and we write:

$$u(x, t) = a \left[1 + \frac{2(\cos[4\sqrt{2}a^2 t] + i\sqrt{2}\sin[4\sqrt{2}a^2 t])}{\cos[4\sqrt{2}a^2 t] + \sqrt{2}\cosh[2ax]} \right] e^{2ia^2 t} \quad (45)$$

A simple graph of this function is shown in Fig. 8. The maximum value of this waveform is $u_{\max}(0, \pi/(4\sqrt{2}a^2)) = 1 + 2\sqrt{2} \cong 3.828$. The temporal period is given by

$$T = \frac{\pi}{2\sqrt{2}a^2} \quad (46)$$

Thus a convenient temporal plotting interval is $(-\pi/(2\sqrt{2}a^2), 0)$. The smallest amplitude occurs at these two intervals. Thus the *large amplitude initial condition* is

$$u(x, t) = a \left[1 + \frac{2}{1 + \sqrt{2}\cosh[2ax]} \right] \quad (47)$$

⁴Some authors refer to the “Kuznetsov-Ma soliton” but I refer to this spectral component in the IST as a breather because that is actually what it is. The soliton solutions to NLS occur far above ia in the λ -plane.

Classification of homoclinic rogue wave solutions

A. R. Osborne

Title Page

Abstract

Introduction

Conclusions

References

Tables

Figures

◀

▶

◀

▶

Back

Close

Full Screen / Esc

Printer-friendly Version

Interactive Discussion



Classification of homoclinic rogue wave solutions

A. R. Osborne

[Title Page](#)

[Abstract](#)

[Introduction](#)

[Conclusions](#)

[References](#)

[Tables](#)

[Figures](#)

◀

▶

◀

▶

[Back](#)

[Close](#)

[Full Screen / Esc](#)

[Printer-friendly Version](#)

[Interactive Discussion](#)



which has exponential tails and rises to the maximum value (at $x = 0$) of ~ 3.828 . Thus an initial condition, for example in the laboratory environment, has this *non-small-amplitude* shape. This allows one to access the complex plane *above the carrier*. Physically there is a great difference between solutions below and above the carrier in the lambda plane. Those below the carrier arise from *small amplitude initial modulations*.

- 5 Those above the carrier arise from *large amplitude initial modulations*. We have learned a great deal about solutions below the carrier using linear instability analysis (Yuen and Lake, 1982). Only by the present *nonlinear instability analysis* using periodic IST have we learned about solutions above the carrier that physically arise from large amplitude initial modulations. These large amplitude initial condition solutions occur for $\lambda_1 > ia$.

10 8 The homoclinic rogue wave packets: relationship to riemann theta functions

The theta function solution to the nonlinear Schrödinger equation is given by (see Osborne (2010) and references):

$$15 u(x, t) = a \frac{\theta(x, t | \mathcal{B}, \delta^-)}{\theta(x, t | \mathcal{B}, \delta^+)} e^{2ia^2 t} \quad (48)$$

where

$$\theta(x, t | \tau, \delta^\pm) = \\ = \sum_{m_1=-\infty}^{\infty} \sum_{m_2=-\infty}^{\infty} \dots \sum_{m_N=-\infty}^{\infty} \exp i \left[\pi \sum_{j=1}^N \sum_{k=1}^N m_j m_k \tau_{jk} \right] \exp i \left[\sum_{n=1}^N m_n K_n x + \sum_{n=1}^N m_n \Omega_n t + \sum_{n=1}^N m_n \delta_n^\pm \right] \quad (49)$$

A leading order in the small parameter ε (a small parameter separating two points of simple spectrum separated by a “spine”) of the loop integrals for the case $N = 2$ (Osborne (2010)) gives the following parameters in the theta function for a two by two Riemann matrix:

20 8.1 Width of expansion parameter and sign of riemann sheet index

$$\varepsilon_1 = \varepsilon_o e^{i\theta} \quad \varepsilon_2 = \varepsilon_1^* \quad (50)$$

$$\sigma_1 = 1 \quad \sigma_2 = -1$$

8.1.1 Spectral eigenvalue

5 $\lambda_1 = \lambda_R + i\lambda_I \quad \lambda_2 = \lambda_1^* \quad (51)$

8.1.2 Spectral wavenumber

$$K_1 = -2\sqrt{a^2 + \lambda_1^2} \quad K_2 = -2\sqrt{a^2 + \lambda_2^2} \quad (52)$$

8.1.3 Spectral frequency

$$\Omega_1 = 2\lambda_1 K_1 \quad \Omega_2 = 2\lambda_2 K_2 \quad (53)$$

10 8.1.4 Period matrix

$$\tau_{11} = \frac{1}{2} + \frac{i}{\pi} \ln \left(\frac{K_1^2}{\varepsilon_1} \right) \quad \tau_{12} = \frac{i}{2\pi} \ln \left(\frac{1 + \lambda_1 \lambda_2 + \frac{1}{4} K_1 K_2}{1 + \lambda_1 \lambda_2 - \frac{1}{4} K_1 K_2} \right) \quad (54)$$

$$\tau_{12} = \frac{i}{2\pi} \ln \left(\frac{1 + \lambda_1 \lambda_2 + \frac{1}{4} K_1 K_2}{1 + \lambda_1 \lambda_2 - \frac{1}{4} K_1 K_2} \right) \quad \tau_{22} = \frac{1}{2} + \frac{i}{\pi} \ln \left(\frac{K_2^2}{\varepsilon_2} \right) \quad (55)$$

NHESSD

2, 897–933, 2014

Classification of
homoclinic rogue
wave solutions

A. R. Osborne

Title Page

Abstract

Introduction

Conclusions

References

Tables

Figures

◀

▶

◀

▶

Back Close

Full Screen / Esc

Printer-friendly Version

Interactive Discussion



8.1.5 Phases

$$\begin{aligned}\delta_1^+ &= \pi + i \ln \left(\lambda_1 - \frac{1}{2} K_1 \right) + i \ln \left(\sigma_1 \lambda_1 + \frac{1}{2} K_1 \right) \\ \delta_1^- &= \pi + i \ln \left(\lambda_1 + \frac{1}{2} K_1 \right) + i \ln \left(\sigma_1 \lambda_1 + \frac{1}{2} K_1 \right) \\ \delta_2^+ &= \pi + i \ln \left(\lambda_2 - \frac{1}{2} K_2 \right) + i \ln \left(\sigma_2 \lambda_2 - \frac{1}{2} K_2 \right) \\ \delta_2^- &= \pi + i \ln \left(\lambda_2 + \frac{1}{2} K_2 \right) + i \ln \left(\sigma_2 \lambda_2 - \frac{1}{2} K_2 \right)\end{aligned}\quad (56)$$

- 5 Use of the above formulas in the theta function provides a simple way to compute the unstable modes and breathers for the particular case of a modulated plane wave carrier. Variable definitions in the λ -plane are shown in Fig. 9 below.

It is clear that insertion of the above Riemann spectrum into the theta functions in (48) gives, in the limit $\varepsilon \rightarrow 0$, the homoclinic solutions discussed herein as a function of
10 the spectral parameters in (50–56). The connections of the parameters used in Eq. (1) to the IST parameters in Eqs. (50–56) are those discussed above.

I would also like to point out that the above formulas, when inserted into the theta function, give numerical results that are *indistinguishable* with those of the breather
15 Eq. (1) above. This is an important result, for indeed one needs to go on to the theta functions themselves for the most general solutions of the NLS equation.

9 The homoclinic rogue wave: relationship to single mode degrees of freedom

I have discussed how a two by two Riemann matrix gives rise to Benjamin-Feir unstable wave packets that are theta function solutions of the 1+1 NLS equation. I have also discussed how the theta functions solutions reduce to the homoclinic solution (1) in

Title Page	
Abstract	Introduction
Conclusions	References
Tables	Figures
◀	▶
◀	▶
Back	Close
Full Screen / Esc	
Printer-friendly Version	
Interactive Discussion	



- 20 an appropriate limit ($\varepsilon \rightarrow 0$). What happens when the Riemann matrix is one by one rather than two by two? The answer is quite simple; the modulations are *stable dnoidal waves*. Let us use this idea from two points of view: (1) the theta function solutions of the NLS equation and (2) the periodic *stable solutions* of NLS.

9.1 The theta functions for dnoidal wave solutions of the NLS equation

- 5 The theta function solution of NLS in one dimension for a one by one Riemann matrix is given by:

$$u(x, t) = a \frac{\theta(x, t | \mathcal{B}, \delta^-)}{\theta(x, t | \mathcal{B}, \delta^+)} e^{2ia^2 t}$$

To see the simple, approximate algebraic form of this stable modulation assume that the nome q is small and we can write:

10 $\theta(x, t | \tau, \pi) \simeq 1 + 2q \cos(kx - \omega t + \pi), \quad q = e^{-\pi\tau}$

The solution to NLS is then given approximately by

$$u(x, t) \simeq a \left(\frac{1 + 2q \cos(kx - \omega t + \pi)}{1 + 2q \cos(kx - \omega t)} \right) e^{2ia^2 t}$$

- Here $q = \exp(-\pi\tau)$, $a = 1$ and $\omega = \sqrt{gk}$. As an example we set $L = 100$ m, then $k = 2\pi/L = 0.06283 \text{ m}^{-1}$ and $\omega = 0.7851 \text{ rad/sec}$, $f = 0.12495 \text{ Hz}$ and $T = 8.003 \text{ s}$. Choose 15 $q = 0.03$, $q = 0.2$ to get the results shown in Figs. 10, 11. Figures 12 and 13 give these two cases, where the carrier wave is also shown.

- Thus we have the full physical interpretation of solutions of the NLS equation. There are two kinds of nonlinear modes: (1) the stable dnoidal wave modulations of Stokes waves for which the Riemann matrix is one by one (which we just discussed) and (2) the unstable Benjamin-Feir modulations of Stokes waves for which the Riemann matrix

[Title Page](#)

[Abstract](#)

[Introduction](#)

[Conclusions](#)

[References](#)

[Tables](#)

[Figures](#)

◀

▶

◀

▶

[Back](#)

[Close](#)

[Full Screen / Esc](#)

[Printer-friendly Version](#)

[Interactive Discussion](#)



is two by two (discussed above and referred to as “breathers”). It should be clear at this juncture that two phase locked dnoidal waves correspond to a breather packet. Large wave packets (extreme waves) are typically of the unstable type and are nearly homoclinic in their spectral structure (Isla and Schober, 2005).

9.2 The Dnoidal Wave Solution as a Stable Mode

- 5 One can find *stationary* periodic solutions of the NLS equation of the type

$$\psi(x,t) = a_o \chi(X) e^{-\frac{i}{2} k_o^2 a_o^2 \omega_o t}, \quad X = x - \left(\frac{\omega_o}{2k_o} \right) t$$

Note that this is just a Galilean transformation from the laboratory coordinate frame to a frame that moves with the group velocity $C_g = \omega_o/2k_o$. Upon substituting the above expression into the space NLS equation we find the ordinary differential equation:

$$10 \quad \frac{\omega_o}{8k_o^2} \chi_{XX} + \sigma^2 \chi + \frac{1}{2} \omega_o k_o^2 \chi^3 = 0$$

This equation can be integrated exactly after multiplying through by the integration factor χ_X . The solutions are the Jacobian elliptic functions of the second kind:

$$\chi(X) = \chi_o d n [\chi_o (X - X_o) | m]$$

This is the dnoidal wave solution of the NLS equation and m is the *elliptic modulus*,
15 $0 \leq m \leq 1$. Also

$$\chi_o = \sigma \sqrt{\frac{2}{(2 - m^2)}}$$

In the limit $m \rightarrow 0$ the solution to the NLS equation becomes the carrier wave

$$\psi(x,t) = a_o e^{-\frac{i}{2} k_o^2 a_o^2 \omega_o t}$$

[Title Page](#)

[Abstract](#)

[Introduction](#)

[Conclusions](#)

[References](#)

[Tables](#)

[Figures](#)

◀

▶

[Back](#)

[Close](#)

[Full Screen / Esc](#)

[Printer-friendly Version](#)

[Interactive Discussion](#)



Classification of homoclinic rogue wave solutions

A. R. Osborne

[Title Page](#)

[Abstract](#)

[Introduction](#)

[Conclusions](#)

[References](#)

[Tables](#)

[Figures](#)

◀

▶

◀

▶

[Back](#)

[Close](#)

[Full Screen / Esc](#)

[Printer-friendly Version](#)

[Interactive Discussion](#)



as expected.

From the theory of Jacobian elliptic functions we know that they are related to the Riemann theta functions. In particular the dnoidal wave has the form (Abramowitz and Stegun, 1963):

$$dn(u) = \frac{\theta_d(u)}{\theta_n(u)} = \frac{\theta_3(v)}{\theta_3(0)} \frac{\theta_4(0)}{\theta_4(v)}, \quad \theta_4(kx) = \theta_3(kx + \pi)$$

so that $\theta_4(0) = \theta_3(\pi)$

$$dn(u) = \frac{\theta_d(u)}{\theta_n(u)} = \frac{\theta_4(0)}{\theta_3(0)} \frac{\theta_3(kx)}{\theta_3(kx + \pi)}, \quad \theta_4(kx) = \theta_3(kx + \pi)$$

Thus we see that this stable solution of the NLS equation is just the dnoidal wave, which is nothing more than the ratio of two theta functions, one phased with respect to the other by π . The dnoidal wave solution is a single-degree of freedom stable Fourier

component of the inverse scattering transform. From Osborne (2010) we know that two simple eigenvalues, one above and the other below the real axis in the λ -plane, connected by a spine corresponds to a dnoidal wave.

10 The dimensional form of the homoclinic solutions

The simple scaled form for the homoclinic solution (1) of the NLS equation (the first equation in this paper) was derived without consideration for applications, where engineering units are useful. To put the above into dimensional form use:

$$u(x, t) \rightarrow \lambda \psi(x, t), \lambda = \sqrt{2k_o^2}; t \rightarrow \beta t, \beta = -\frac{\omega_o}{8k_o^2}; a \rightarrow \lambda a_o \quad (57)$$

we could also carry out the Galilean transformation $x \rightarrow x - C_g t$ to get back to the laboratory frame of reference, but I do not do that here. The important thing here is that

20 x is not scaled. Now use $a \rightarrow \lambda a_o$ and get for (1)

$$\lambda\psi(x,t) = -i\lambda a_o \left(\frac{1 - 2\cos(Kx)e^{\Omega\beta t - 2i\phi + \gamma} + Ae^{2\Omega\beta t - 4i\phi + 2\gamma}}{1 - 2\cos(Kx)e^{\Omega\beta t + \gamma} + Ae^{2\Omega\beta t + 2\gamma}} \right) e^{2ia^2 t} \quad (58)$$

This suggests that we need to set $\Omega\beta \rightarrow \Omega$, so that:

$$\lambda\psi(x,t) = -i\lambda a_o \left(\frac{1 - 2\cos(Kx)e^{\Omega\beta t - 2i\phi + \gamma} + Ae^{2\Omega\beta t - 4i\phi + 2\gamma}}{1 - 2\cos(Kx)e^{\Omega\beta t + \gamma} + Ae^{2\Omega\beta t + 2\gamma}} \right) e^{2ia^2 t} \quad (59)$$

where

$$5 \quad \Omega = \beta K \sqrt{4\lambda^2 a_o^2 - K^2} = 2\lambda a_o \beta K \sqrt{1 - \left(\frac{K}{2\sqrt{\lambda} a_o} \right)^2}$$

is the modulation frequency, which in dimensional form is:

$$\Omega = \beta K \sqrt{4\lambda^2 a_o^2 - K^2} = 2\sqrt{2} k_o^2 a_o \frac{\omega_o}{8k_o^2} K \sqrt{1 - \left(\frac{K}{2\sqrt{2} k_o^2 a_o} \right)^2}$$
$$\Omega = k_o^2 a_o^2 \omega_o \left(\frac{K}{2\sqrt{2} k_o^2 a_o} \right) \sqrt{1 - \left(\frac{K}{2\sqrt{2} k_o^2 a_o} \right)^2} \quad (60)$$

10 This is the Yuen result for dimensional NLS, for which the dimensional solution follows. Here I use the minus sign in the expression for $\beta = -\omega_o/8k_o^2$ and neglected the $-i$, which is just an arbitrary phase. We finally have for *dimensional results for the general homoclinic solution of the dimensional NLS equation*:

$$\psi(x,t) = a_o \left(\frac{1 - 2\cos(Kx)e^{-\Omega t - 2i\phi + \gamma} + Ae^{-2\Omega t - 4i\phi + 2\gamma}}{1 - 2\cos(Kx)e^{-\Omega\beta t + \gamma} + Ae^{-2\Omega\beta t + 2\gamma}} \right) e^{-\frac{1}{2}ik_o^2 a_o^2 \omega_o t} \quad (61)$$

Title Page

Abstract

Introduction

Conclusions

References

Tables

Figures

◀

▶

Back

Close

Full Screen / Esc

Printer-friendly Version

Interactive Discussion



$$\Omega = k_o^2 a_o^2 \omega_o \left(\frac{K}{2\sqrt{2}k_o^2 a_o} \right) \sqrt{1 - \left(\frac{K}{2\sqrt{2}k_o^2 a_o} \right)^2} \quad (62)$$

$$K = 2\sqrt{2}k_o^2 a_o \sin \phi \quad (63)$$

$${}^5 L = \frac{2\pi}{K} = \frac{\pi}{\sqrt{2}k_o^2 a_o \sin \phi} \quad (64)$$

$$a_o = \frac{1}{\cos^2 \phi} \quad (65)$$

Now let's connect this solution to the IST eigenvalue in the lambda plane. Recall the expression for the modulation wavenumber to order ε (Osborne, 2010):

$${}^{10} \frac{K}{2\sqrt{2}k_o^2 a_o} = \sqrt{1 - \left(\frac{\lambda_I}{2\sqrt{2}k_o^2 a_o} \right)^2} \quad (66)$$

$$\left(\frac{K}{2\sqrt{2}k_o^2 a_o} \right)^2 + \left(\frac{\lambda_I}{2\sqrt{2}k_o^2 a_o} \right)^2 = 1 \quad (67)$$

and the inverse:

$$\frac{\lambda_I}{2\sqrt{2}k_o^2 a_o} = \sqrt{1 - \left(\frac{K}{2\sqrt{2}k_o^2 a_o} \right)^2} \quad (68)$$

Classification of homoclinic rogue wave solutions

A. R. Osborne

[Title Page](#)

[Abstract](#)

[Introduction](#)

[Conclusions](#)

[References](#)

[Tables](#)

[Figures](#)

◀

▶

◀

▶

[Back](#)

[Close](#)

[Full Screen / Esc](#)

[Printer-friendly Version](#)

[Interactive Discussion](#)



15 This suggests introduction of the angle ϕ :

$$\frac{\lambda_1}{2\sqrt{2}k_o^2a_o} = \cos\phi, \quad \frac{K}{2\sqrt{2}k_o^2a_o} = \sin\phi \quad (69)$$

We also have

$$\frac{\lambda_1}{2\sqrt{2}k_o^2a_o} = \cos\phi = \frac{1}{\sqrt{a}}$$

Figure 14 gives the dimensional form of the equations in the lambda plane.

5 11 Conclusions

I have discussed how the general periodic solutions of the NLS equation, in terms of Riemann theta functions, with a two by two Riemann matrix ($N = 2$), can be reduced to the associated homoclinic solutions in an appropriate limit ($\varepsilon \rightarrow 0$). The homoclinic solutions contain the Akhmediev, Peregrine and Kuznetsov-Ma cases for the λ -plane

10 eigenvalues $\lambda_1 = ia_o/\sqrt{2}$, $\lambda_1 = ia_o$ and $\lambda_1 = i\sqrt{2}a_o$ respectively. These three solutions have been used in the Extreme Seas program for engineering purposes. I suggest that the other infinity of solutions, as parameterized in engineering units in Eqs. (61–65), over the *entire* complex λ -plane, could also be used to develop engineering design procedures.

15 The solutions found by Matveev and colleagues (Dubard, Gaillard, Klein and Matveev, 2010) (Dubard and Matveev, 2011) correspond to the case $N = 4$ are associated with a four by four Riemann matrix with appropriate phase locking. I will discuss these in detail with relation to the periodic IST in a later publication.

20 *Acknowledgements.* This work was conducted under the auspices of the research wing of Nonlinear Waves Research Corp, for which the author is grateful for support. While some of the material of my course on *Nonlinear Waves* at the University of Torino over the past 30 years

Title Page

Abstract

Introduction

Conclusions

References

Tables

Figures

◀

▶

Back

Close

Full Screen / Esc

Printer-friendly Version

Interactive Discussion



has become available during the Extreme Seas program, the material given herein seems to have been overlooked. I have therefore discussed the results here, in a somewhat didactical vein, in the hope that the material will be found useful in the ship design problem, for Extreme Seas participants and others. I am also grateful to D. Faulkner who suggested that this work be carried out: His foresight led to the MaxWave and Extreme Seas programs.

5 References

- Abramowitz, M. and Stegun, I. A.: Handbook of Mathematical Functions. National Bureau of Standards, Appl. Math. Ser. 55, 1964.
- Akhmediev, N.: Teoreticheskaya i Matematicheskaya Fizika, 69, 189–194, 1986.
- Akhmediev, N. and Pelinovsky, E.: Discussion and Debate: Rogue Waves – Towards a Unifying Concept? The European Physical Journal Special Topics, Volume 185, Issue 1, July 2010.
- Belokolos, E. D., Bobenko, A. I., Enolskii, V. Z., Its, A. R., and Matveev, V. B.: Algebro- Geometric Approach to Nonlinear Integrable Equations, Springer-Verlag, Berlin, 1994.
- Dubard, P., Gaillard, P., Klein, C., and Matveev, V. B.: On multi-rogue wave solutions of the NLS equation and positon solutions of the KdV Equation, Eur. Phys. J. Special Topics, 185, 247–258, 2010.
- Dubard, P. and Matveev, V. B.: Multi-rogue waves solutions to the focusing NLS equation and the KP-I equation, Nat. Hazards Earth Syst. Sci., 11, 667–672, doi:10.5194/nhess-11-667-2011, 2011.
- Faulkner, D.: Defining Rogue Waves for Marine Design, proceedings of a workshop: Rogue Waves 2000, edited by: Olagnon, M. and Athanassoulis, G. A., 2000.
- Ilas, A. L. and Schober, C. M.: Predicting rogue waves in random oceanic sea states, Physics of Fluids, Volume 17, Issue 3, 031701-031701-4, 2005.
- Kharif, C., Pelinovsky, E., and Slunyaev, A.: Rogue Waves in the Ocean, Springer-Verlag, Berlin, 2009.
- Kotlyarov, V. P. and Its, A. R.: Dopovidi Akad. Nauk. UkrSR., Serie A, Vol. 11, 965–968, 1976, (in Ukrainian)
- Kuznetsov, E.: Solitons in a parametrically unstable plasma, Sov. Phys. Dokl., 22, 507–508, 1977.

Title Page	
Abstract	Introduction
Conclusions	References
Tables	Figures
◀	▶
◀	▶
Back	Close
Full Screen / Esc	
Printer-friendly Version	
Interactive Discussion	



Classification of homoclinic rogue wave solutions

A. R. Osborne

- Ma, Y. C.: The perturbed plane-wave solutions of the cubic Schrödinger equation, *Stud. Appl. Math.* 60, 43, 1979.
- Olagnon, M. and Athanassoulis, G. A.: Rogue Waves 2000, Ifremer, Brest, 2000.
- Olagnon, M. and Prevost, M.: Rogue Waves 2004, Ifremer, Brest, 2004.
- Olagnon, M. and Prevost, M.: Rogue Waves 2008, Ifremer, Brest, 2008.
- Osborne, A. R.: Rogue Waves: Classification, measurement and data analysis, and hyperfast numerical modeling, *Eur. Phys. J. Special Topics*, 185, 225–245, 2010.
- Osborne, A. R.: Nonlinear Ocean Waves and the Inverse Scattering Transform. Academic Press, International Geophysics Series Volume 97, Boston, 944 pages, 2010.
- Osborne, A. R.: Deterministic and Wind/Wave Modeling: A Comprehensive Approach To Deterministic and Probabilistic Descriptions of Ocean Waves, Proceedings of the 31st International Conference on Ocean, Offshore and Arctic Engineering OMAE2012 June 10-15, 2012, Rio de Janeiro, Brazil.
- Osborne, A. R.: Advances in Nonlinear Waves with Emphasis on Aspects for Ship Design and Wave Forensics, Proceedings of the ASME 2013 32nd International Conference on Ocean, Offshore and Arctic Engineering OMAE2013 June 9-14, 2013, Nantes, France.
- Pelinovsky, E. and Kharif, C.: Extreme Ocean Waves, Springer-Verlag, Berlin, 2008.
- Peregrine, D. H.: Water waves, nonlinear Schrödinger equations and their solutions, *J. Aust. Math. Soc. B*, 16–43, 1983.
- Yuen H. C. and Lake, B. M.: Nonlinear dynamics of deep-water gravity waves, *Adv. Appl. Mech.* 22, 67–229, 1982.

[Title Page](#)[Abstract](#)[Introduction](#)[Conclusions](#)[References](#)[Tables](#)[Figures](#)[|◀](#)[▶|](#)[Back](#)[Close](#)[Full Screen / Esc](#)[Printer-friendly Version](#)[Interactive Discussion](#)

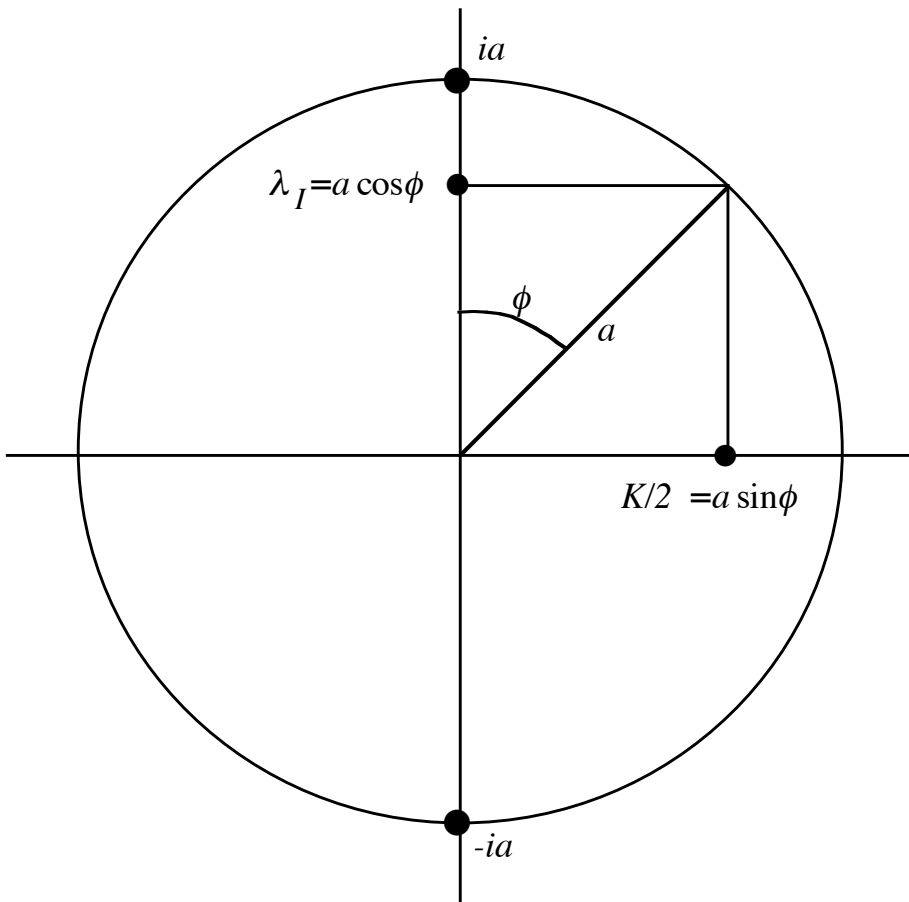


Fig. 1. Geometry of parameters for a homoclinic, unstable mode below the carrier in the λ -plane. Here λ_1 lies on the interval $(0, ia)$.

Classification of homoclinic rogue wave solutions

A. R. Osborne

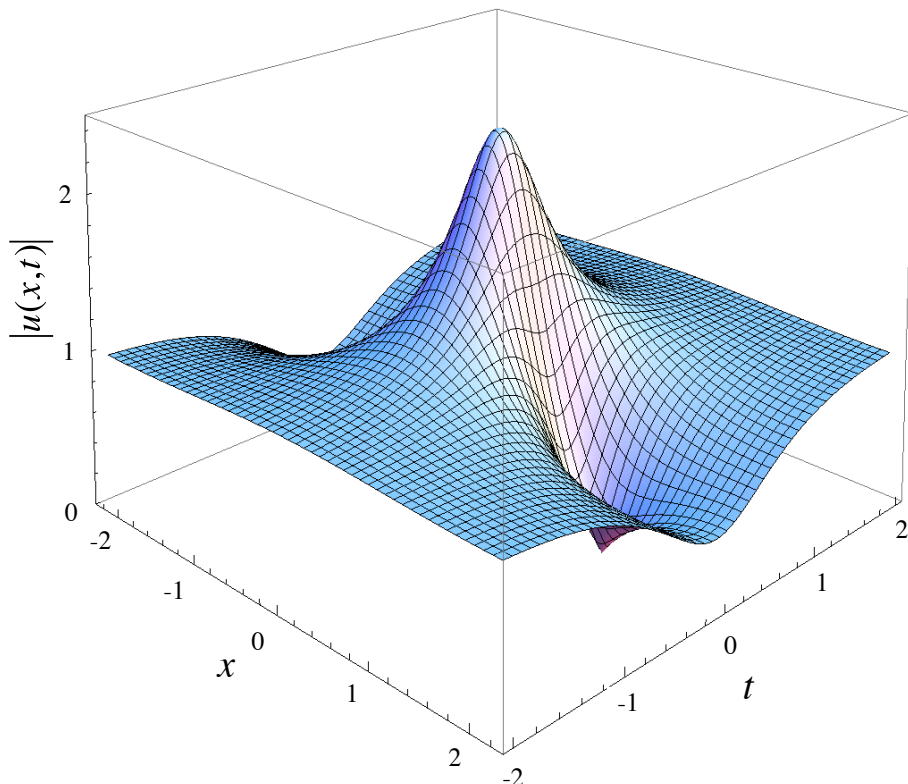


Fig. 2. Modulus of the rogue wave Akhmediev breather solution (21) as a function of space and time.

- [Title Page](#)
- [Abstract](#) [Introduction](#)
- [Conclusions](#) [References](#)
- [Tables](#) [Figures](#)
- [◀](#) [▶](#)
- [◀](#) [▶](#)
- [Back](#) [Close](#)
- [Full Screen / Esc](#)
- [Printer-friendly Version](#)
- [Interactive Discussion](#)



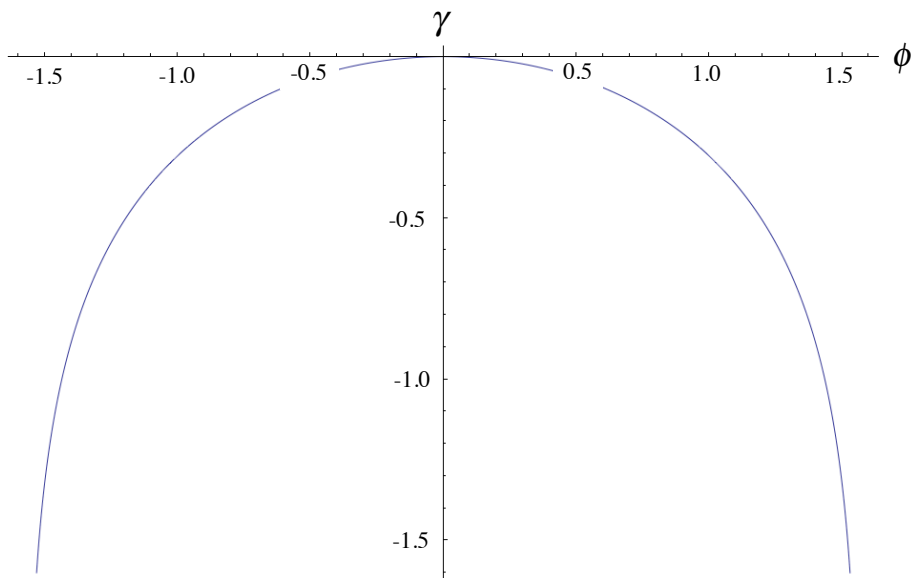


Fig. 3. Graph of γ as a function of ϕ , $\gamma = \ln(\cos \phi)$, for the simplified reduced rogue wave (25).

**Classification of
homoclinic rogue
wave solutions**

A. R. Osborne

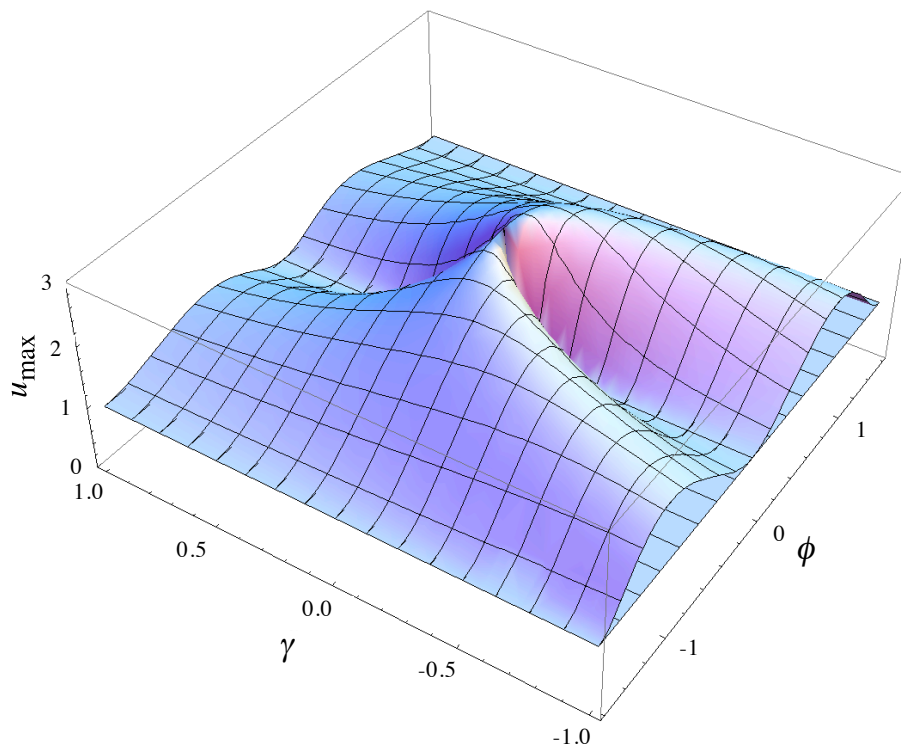


Fig. 4. Graph of the rogue wave maximum, $|u(0,0)|(\phi, \gamma)$, as a function of ϕ , γ .

Classification of homoclinic rogue wave solutions

A. R. Osborne

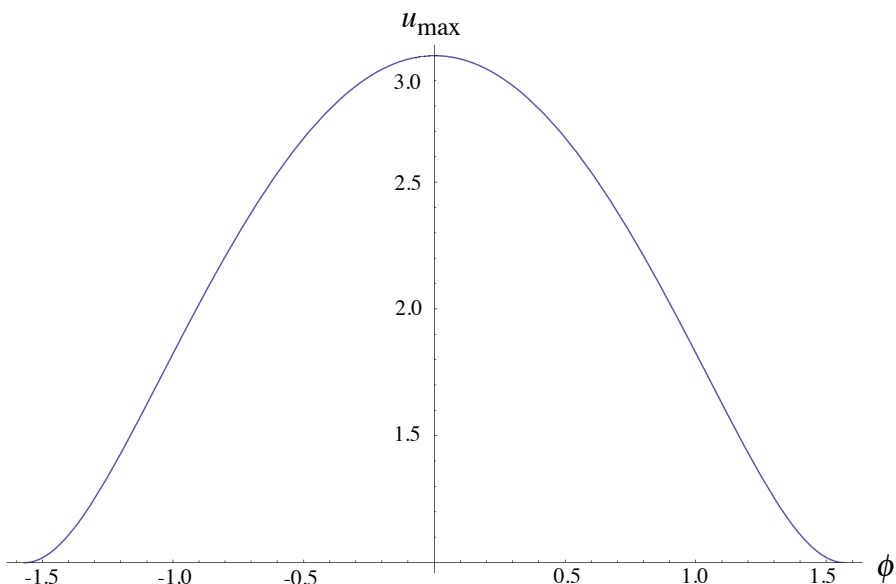


Fig. 5. Graph of the rogue wave maximum, $|\psi(0,0)|(\phi, 0)$, for $\gamma = 0$.

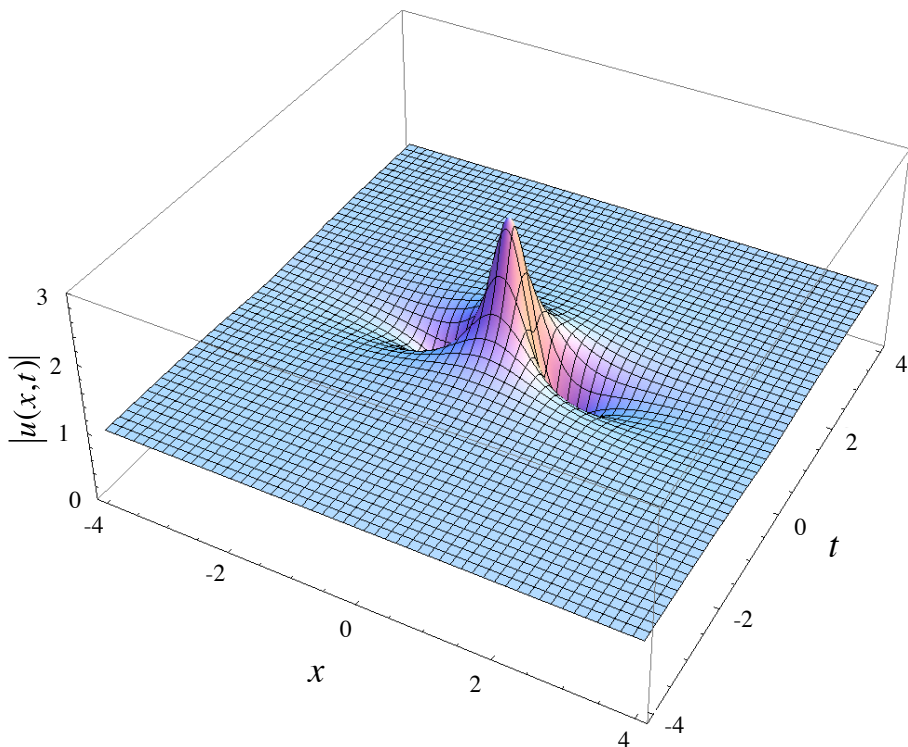


Fig. 6. Graph of the Peregrine solution of the NLS equation.

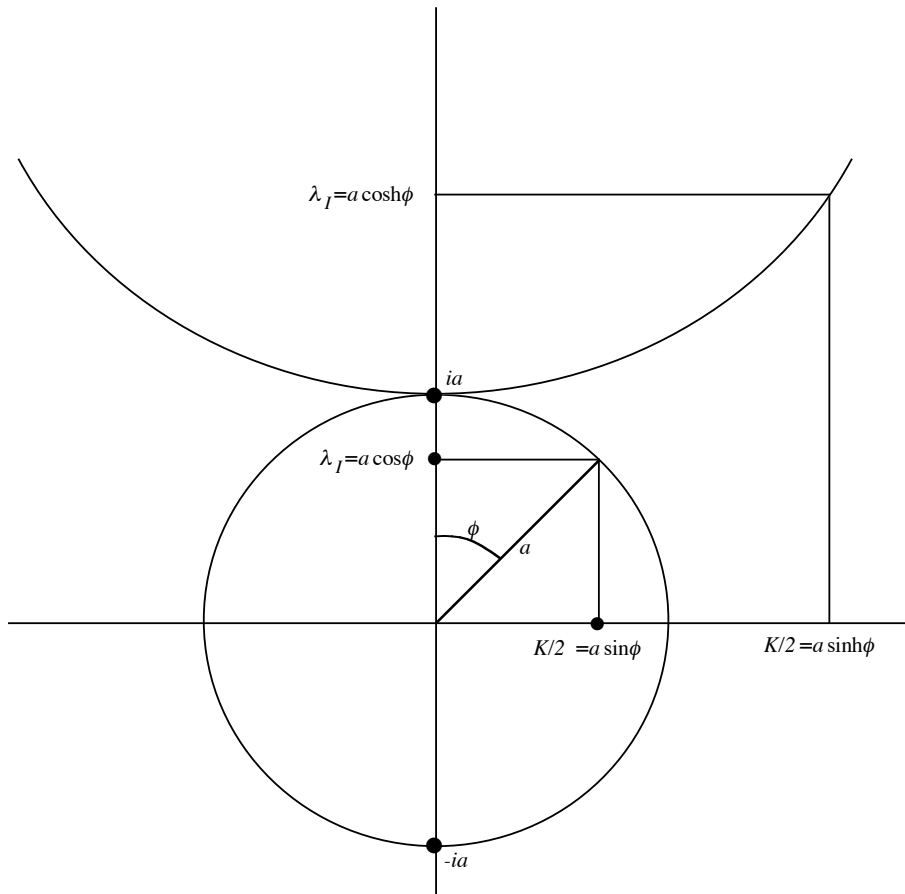


Fig. 7. Geometry of parameters for a homoclinic, unstable mode above the carrier in the lambda plane, i.e. where λ_1 lies on the interval $(ia, i\infty)$.

Classification of homoclinic rogue wave solutions

A. R. Osborne

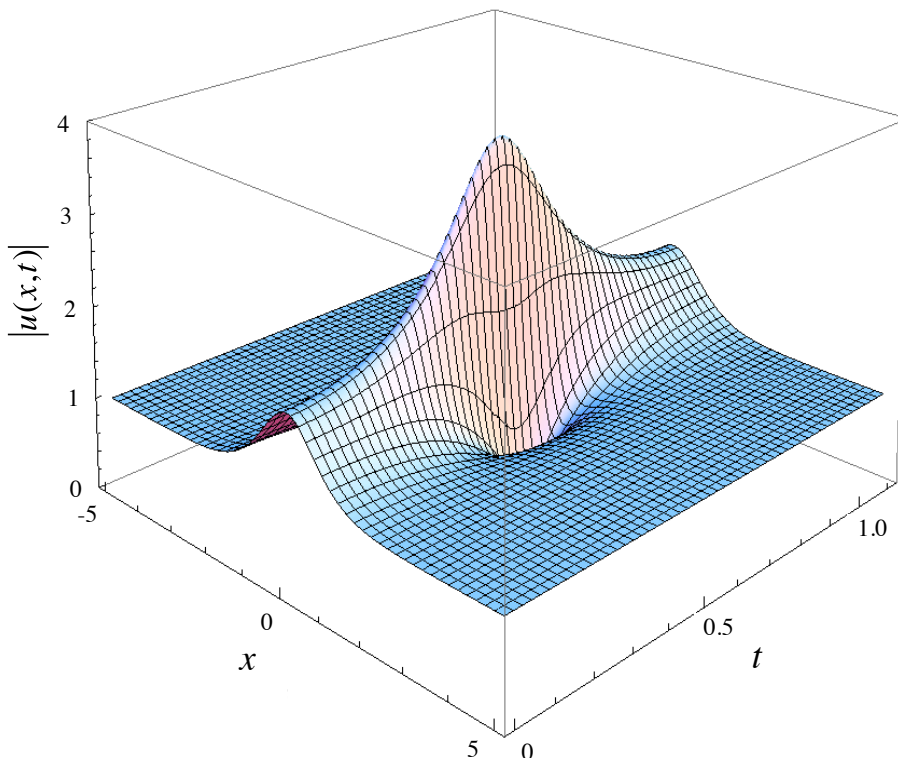


Fig. 8. Graph of the solution of the NLS equation for $\lambda_1 = ia\sqrt{2}$. This is the Ma-Kuznetsov breather.

- [Title Page](#)
- [Abstract](#) [Introduction](#)
- [Conclusions](#) [References](#)
- [Tables](#) [Figures](#)
- [◀](#) [▶](#)
- [◀](#) [▶](#)
- [Back](#) [Close](#)
- [Full Screen / Esc](#)
- [Printer-friendly Version](#)
- [Interactive Discussion](#)

Classification of homoclinic rogue wave solutions

A. R. Osborne

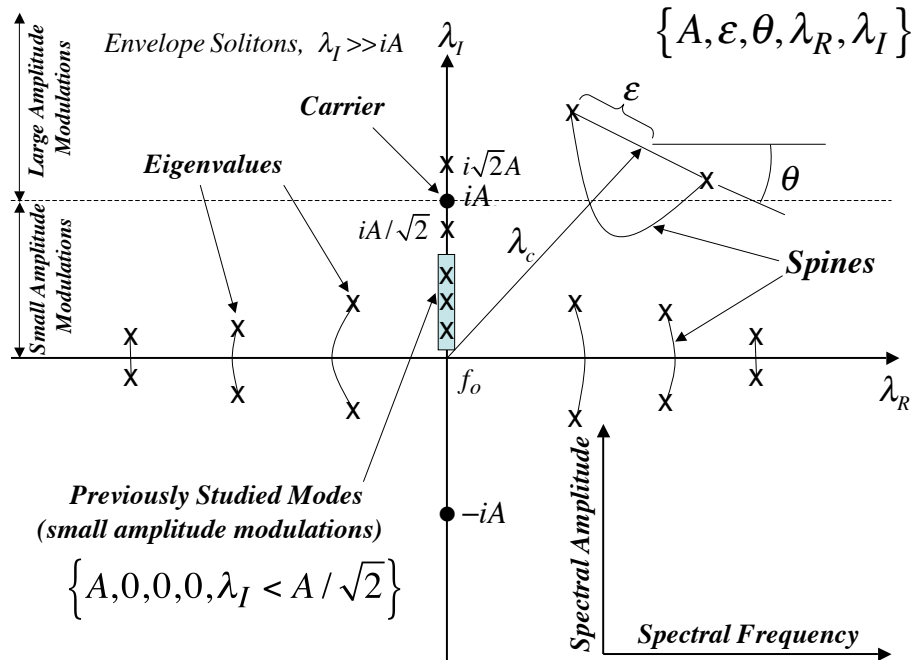


Fig. 9. Lambda plane for spectral solutions of the NLS equation. Only when the spines do not cross the real axis and in the limit $\varepsilon \rightarrow 0$ do we have homoclinic solutions.

Classification of homoclinic rogue wave solutions

A. R. Osborne

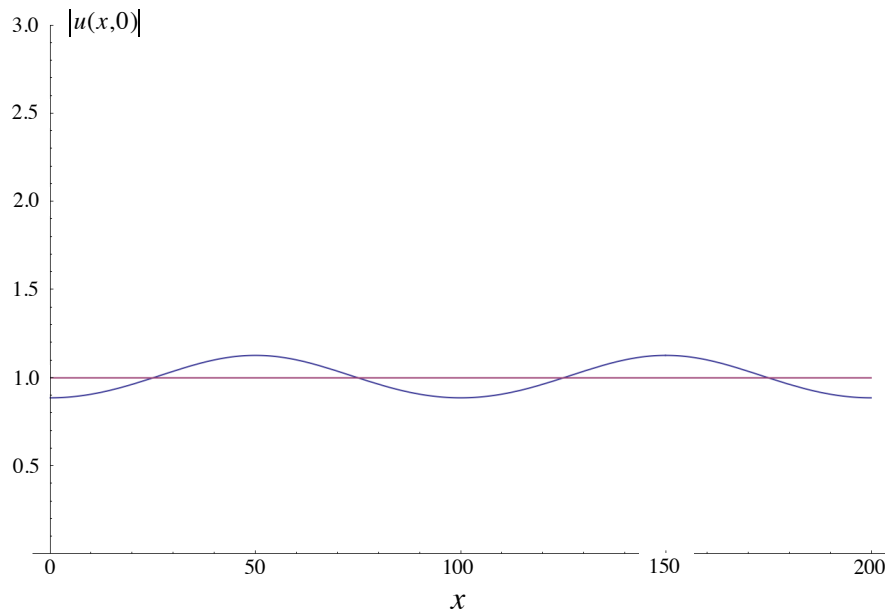


Fig. 10. Stable dnoidal wave modulation of NLS equation for $q = 0.03$.

- [Title Page](#)
- [Abstract](#) [Introduction](#)
- [Conclusions](#) [References](#)
- [Tables](#) [Figures](#)
- [◀](#) [▶](#)
- [◀](#) [▶](#)
- [Back](#) [Close](#)
- [Full Screen / Esc](#)
- [Printer-friendly Version](#)
- [Interactive Discussion](#)



Classification of homoclinic rogue wave solutions

A. R. Osborne

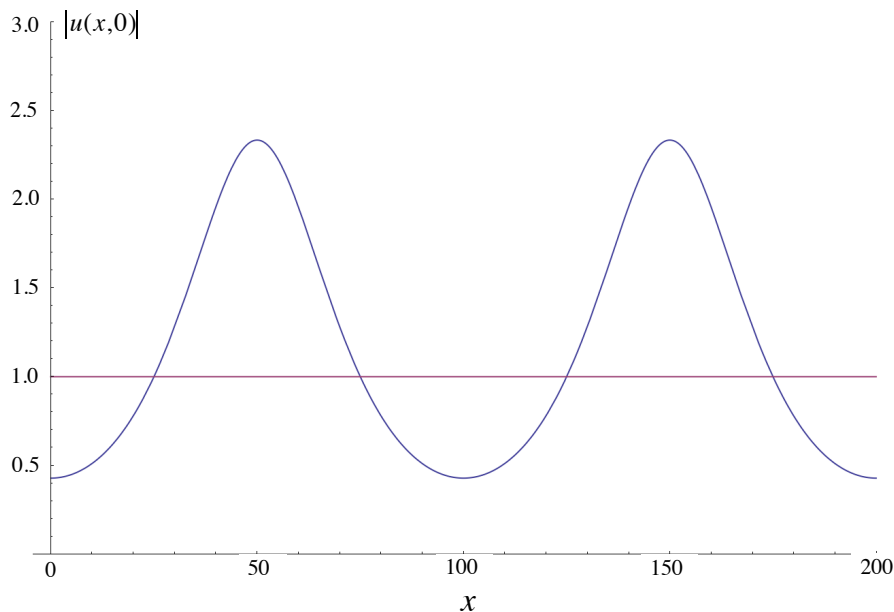


Fig. 11. Stable dnoidal wave modulation of NLS equation for $q = 0.2$.

- [Title Page](#)
- [Abstract](#) [Introduction](#)
- [Conclusions](#) [References](#)
- [Tables](#) [Figures](#)
-
-
- [Full Screen / Esc](#)
- [Printer-friendly Version](#)
- [Interactive Discussion](#)



Classification of homoclinic rogue wave solutions

A. R. Osborne

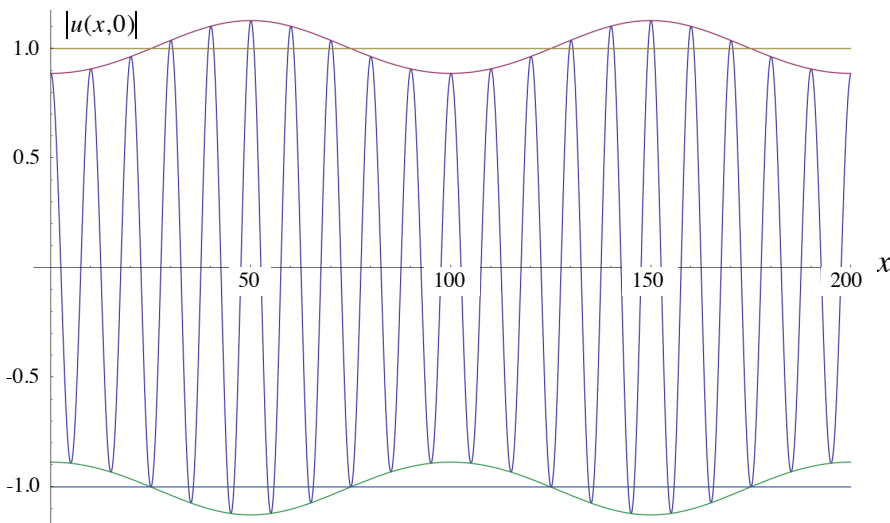


Fig. 12. Stable dnoidal wave modulation of NLS carrier for $q = 0.03$. Shown also is the carrier wave.

- [Title Page](#)
- [Abstract](#) [Introduction](#)
- [Conclusions](#) [References](#)
- [Tables](#) [Figures](#)
- [◀](#) [▶](#)
- [◀](#) [▶](#)
- [Back](#) [Close](#)
- [Full Screen / Esc](#)
- [Printer-friendly Version](#)
- [Interactive Discussion](#)

Classification of homoclinic rogue wave solutions

A. R. Osborne

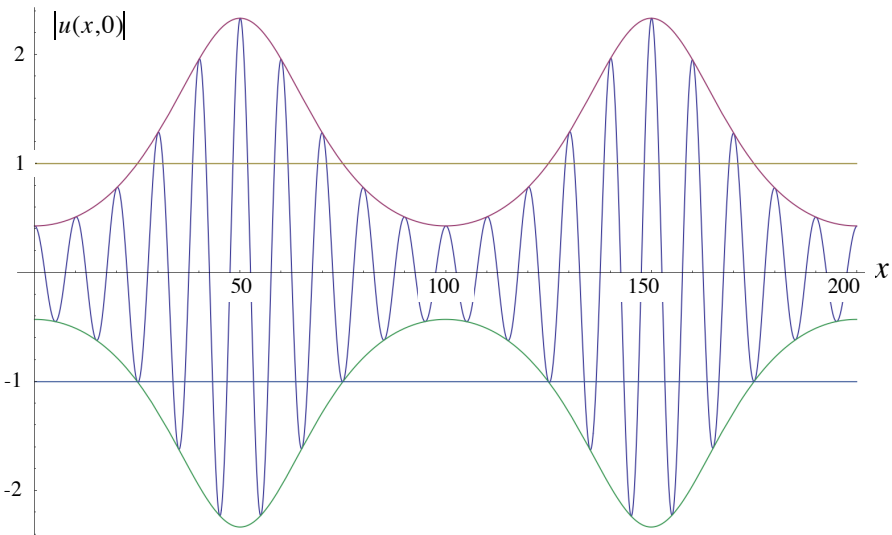


Fig. 13. Stable dnoidal wave modulation of NLS carrier for $q = 0.2$. Shown also is the carrier wave.

[Title Page](#)[Abstract](#)[Introduction](#)[Conclusions](#)[References](#)[Tables](#)[Figures](#)[◀](#)[▶](#)[◀](#)[▶](#)[Back](#)[Close](#)[Full Screen / Esc](#)[Printer-friendly Version](#)[Interactive Discussion](#)

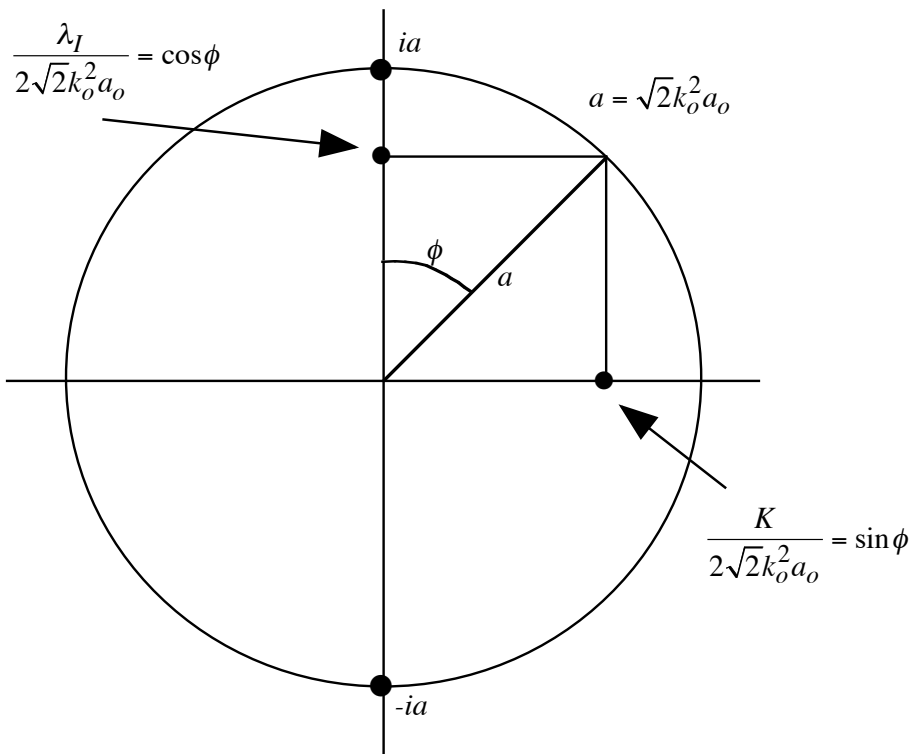


Fig. 14. Spectral parameters for dimensional unstable mode solutions of the NLS equation beneath the carrier.